

# Selective Cold Welding of Colloidal Gold Nanorods

Simona C. Laza,\* Nicolas Sanson,\* Cécile Sicard-Roselli, Anthony Aghedu, and Bruno Palpant

After experiencing great advances in the synthesis of nanoparticles (NPs) with controlled size, shape, and composition, the research in the field of NPs faces a new challenge: the controlled self-assembly of anisotropic NPs with well-defined orientation.<sup>[1]</sup> The interest for this topic lies in the new properties exhibited by the NP assembly as a result of the coupling effects between its individual constituents. The size and shape of the NPs as well as their spatial orientation influence these effects. Especially, the modification of the NP shape opens interesting outlooks for optical applications.<sup>[2]</sup>

For the last years, an extensive research effort has been dedicated to the self-assembly of gold nanorods (AuNRs) due to the special coupling effects of their longitudinal plasmon resonance (LPR).<sup>[3]</sup> The coupling is very sensitive to the nanorod (NR) spatial arrangement, the inter-nanorod distance, the number of NRs participating to the assembly, and also to the geometrical characteristics of each NR.<sup>[4]</sup> This dependence makes LPR the ideal tool to monitor and study the assembling process of AuNRs. Previously reported works use AuNRs with small organic ligands or polymers attached on their surface with a sulfur bonding, and exploit, either the solvent selectivity, or the site-specific interaction of the ligands stabilizing the NRs to achieve their self-assembling.<sup>[5,6]</sup>

Besides, there is also an increasing interest for the NP welding. This interest is driven by both the fundamental aspect of the phenomena leading to the welding of nano-objects<sup>[7,8]</sup> and the potential application of the nanoscale welding to the bottom-up fabrication.<sup>[9]</sup> There exists two types of welding: the hot welding and the cold welding. The hot welding involves the presence of a molten phase resulted from the heating of the parts to be joined, which are then coalesced and solidified.<sup>[10]</sup>

No molten phase is involved in the cold welding. For the bulk metals, the cold welding takes place whenever two atomically clean, flat, ductile surfaces are put in contact, generally under conditions of ultra-high-vacuum or/and high applied normal load.<sup>[8]</sup> At the nanoscale, Whitesides and co-workers<sup>[11]</sup> realized the cold welding of two gold thin films on polydimethylsiloxane substrates under ambient conditions and without any load. For the cold welding of chemically produced NPs, the key is the removal of the NP-capping molecules. Having an uncapped surface increases the NP surface energy and hence favors their coalescence. The cleaning of the NP surface is usually realized by heating (below the melting temperature),<sup>[7]</sup> or by the action of a mechanical force.<sup>[8]</sup>

Herein, we report the formation of micrometric length gold nanowires by selective self-organization and cold welding of as-made cetyltrimethylammonium bromide (CTAB)-stabilized AuNRs in aqueous solution induced by a poly(ethylene oxide-*st*-propylene oxide) copolymer, poly(EO-*st*-PO).

**Figure 1** (Figure S1, Supporting Information) shows the kinetics of the optical absorbance spectrum of the NR solution after the addition of copolymer M1000 (respectively M600). The kinetics presents the typical characteristics of an end-to-end (*E-to-E*) assembly of AuNRs: the transverse plasmon resonance, here at 512 nm, remains unaltered, and the LPR of the isolated AuNRs (here at 675 nm, corresponding to a NR aspect ratio of 2.6) decreases while new coupled modes appear in the red part of the spectral domain (here at 780 nm and around 900 nm).<sup>[3]</sup>

In the very first moments, the peak evolution is clearly dominated by the decrease of the LPR of isolated NRs, correlated with the increase of the peak at 780 nm (Figure 1a,c, and Figure S1a,c, Supporting Information). The presence of an isosbestic point, here at 725 nm (Figure 1a and Figure S1a, Supporting Information), indicates that, at this stage, the AuNRs are present in the solution mainly in two forms.<sup>[12]</sup> The spectral characteristics of our isolated NRs (LPR at 675 nm) correspond well to the ones of the NRs used in the works of Funston et al.<sup>[13]</sup> (LPR between 612 and 678 nm). Moreover, the locations of the third and fourth peaks are in the spectral ranges corresponding to the peaks measured by these authors for *E-to-E* dimers (from 700 to 800 nm) and *E-to-E* trimers (from 800 to 900 nm), respectively.<sup>[13,14]</sup> According to **Figure 2a,b**, which show the transmission electron microscopy (TEM) images of the species present in solution at instants when the new peaks start to be visible, the formation of NR dimers is correlated with the development of the 780 nm peak, while the appearance of NR trimers gives birth to the band at 900 nm. The latter rises later than the former, and it is clearly visible only when the peak at 780 nm approaches its maximum (Figure 1c and Figure S1c, Supporting Information). The magnitude increase of the fourth peak is correlated with the disappearance of the isosbestic point, and hence to the presence in solution of NRs under

Dr. S. C. Laza, A. Aghedu, Prof. B. Palpant  
Ecole Centrale Paris, Laboratoire de  
Photonique Quantique et Moléculaire  
UMR 8537 – CNRS  
Ecole Normale Supérieure du Cachan  
Grande Voie des Vignes  
Châtenay-Malabry, 92295 cedex, France  
E-mail: simona-cristina.laza@ecp.fr

Dr. N. Sanson  
Physicochimie des Polymères et Milieux  
Dispersés-Sciences et Ingénierie de la Matière Molle  
UMR7615, UPMC Sorbonne Universités  
ESPCI Paristech, CNRS, 10 rue Vauquelin,  
75231, Paris cedex 05, France  
E-mail: nicolas.sanson@espci.fr

Dr. C. Sicard-Roselli  
Laboratoire de Chimie Physique  
CNRS UMR 8000, Université Paris-Sud,  
91405, Orsay cedex, France



DOI: 10.1002/ppsc.201300026

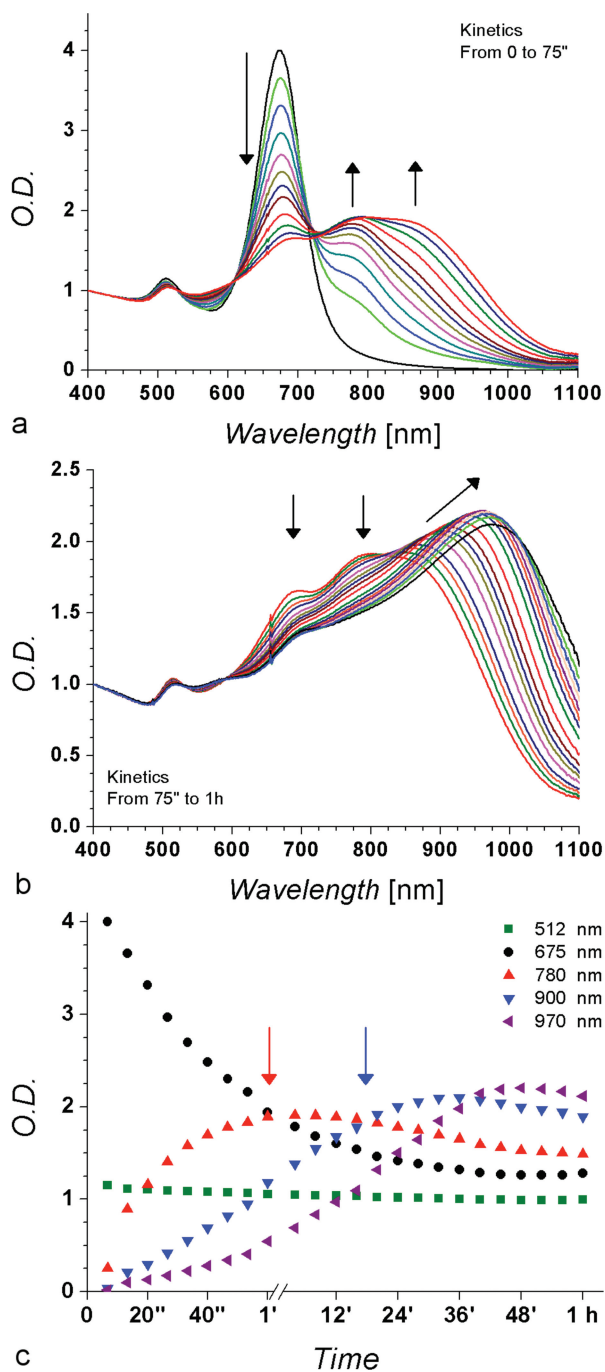


**Figure 1.** Kinetics of the optical absorbance spectrum of the gold NR assembly, a) from 0 to 75 s, spectra recorded each 5 s and b) spectra recorded each 3 min from 75 s to 1 h after the addition of M1000 copolymer. c) Time evolution of the magnitude of the different absorbance peaks after the addition of M1000 copolymer into the NR solution. In a and b, some of the intermediary spectra are skipped for the sake of plot clearness. The arrows in a and b represent the evolution trends of the absorbance peaks, while in c, the arrows represent the instants at which the magnitude of a new peak becomes predominant. The symbols: " , ' , and h stand for seconds, minutes and hours, respectively.

other forms than monomers and dimers. Therefore, we deduce that at early stage of the kinetics the NRs are mainly under the form of isolated NRs and dimers. Moreover, the absence of a

blueshift in the LPR and of any redshift of the TPR of the isolated NRs (Figure 1a,b) indicate that no side-to-side assembly of the NRs takes place.<sup>[3,12,13]</sup>

In the second part of the kinetics (Figure 1b and Figure S1b, Supporting Information), the decrease of the LPR of isolated NRs is accompanied by the decrease of the peak at 780 nm, indicating a decrease in the concentration of isolated NRs and NR dimers, respectively. In the same time, the 900 nm band redshifts, broadens, and its magnitude increases. The TEM images, together with the absorbance kinetics, show the correlation of the bathochromic shift of the 900 nm peak with the formation of longer chains of NRs (Figure 2c–e). The evolution of the third and fourth peaks agrees well also with the results of Wang et al.<sup>[15]</sup> demonstrating that the formation of longer chains takes place only when the monomers have largely been consumed. The new assemblies will then have as building blocks not only monomers but also dimers. On this basis, it is likely that the appearance of the 900 nm peak accounts for the formation of trimers, while its redshift and broadening are ascribed to the formation of even longer chains.

The kinetic studies of the absorbance spectra, correlated with the electron microscopy analysis of the sample at the instants when the new peaks start to be visible, lead us to the conclusion that the addition of polymer solution induces the self-organization of the AuNRs in water, mainly into an *E-to-E* configuration. The TEM images of the solution at the end of the kinetics (when a "steady" spectrum is established), Figure 2f, reveal chains of micrometric length, formed of *E-to-E* assembled NRs.

Figure 2g–j shows HR-TEM details of the junctions between the NRs forming the micrometric chains. The assembled NRs are not only in contact one with the other, but they are welded together. We observe two main configurations of *E-to-E* welding of colloidal AuNRs. One is the twined *E-to-E* welding, which presents a certain angle between the longitudinal directions of the welded NRs (Figure 2g,h) forming a twined crystal. The second is the perfect *E-to-E* welding with zero angle between the longitudinal directions of the NRs, which form a single-crystal structure (Figure 2i,j). The redistribution of Au atoms along the interface between the NRs, as can be observed in Figure 2, indicates a cold welding by oriented attachment (OA).<sup>[8]</sup>

It is known that the OA is a process in which the nanoparticles have to be coaligned before they coalesce.<sup>[8]</sup> Their alignment is attributed to dipole interactions, and the bare metal nanoparticles are known to have strongly attractive van der Waals forces.<sup>[16]</sup> Moreover, for the process of OA to take place between colloidal nanoparticles, the colloidal stabilization must be sufficiently weak to allow them to approach each other down to a distance where van der Waals interactions could lead to further attraction.<sup>[8]</sup>

The welding of two NRs gives birth to a new NR of higher aspect ratio and hence results in the redshift of the LPR. For the NRs used in this work, the welding of a perfect *E-to-E* dimer will result in an NR with an aspect ratio around 5.2 (or a little bit less, depending on the atom redistribution at the junction). AuNRs with aspect ratio around 5.2 exhibit a LPR around 900 nm.<sup>[17]</sup> The typical time needed for the NPs to get in touch by oriented attachment is known to be of the order of a few seconds.<sup>[8]</sup> This is the same time scale as for the appearance of the new absorbance peaks (Figure 1a) in the first part of the kinetics. It follows that in the solution, the NR assembling

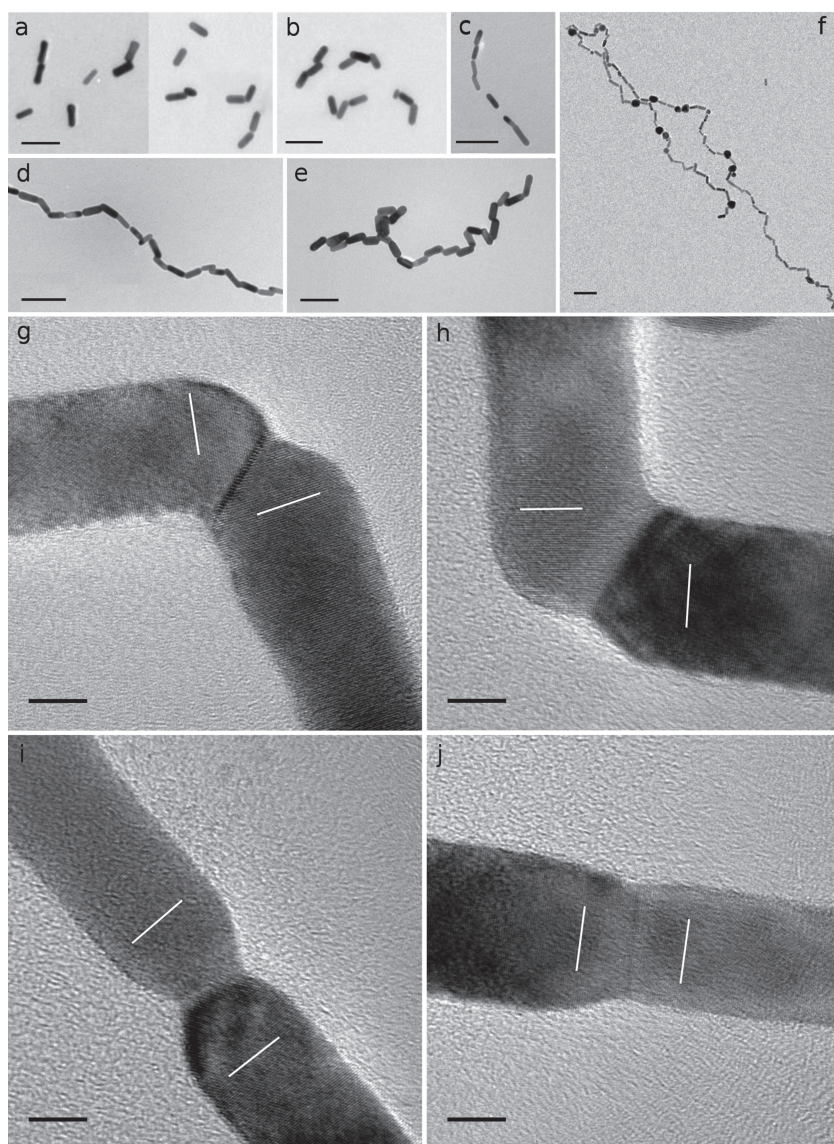


**Figure 2.** a–f) Representative TEM images of the AuNR solution corresponding to different moments of the absorbance spectrum kinetics after the addition of the copolymer solution: a) the peak at 780 nm is clearly visible, b) the peak at 900 nm begins to be well defined, c–e) bathochromic shift of the 900 nm peak, and f) micrometric length NR chains corresponding to the end of the kinetics. g–j) High-resolution transmission electron microscopy (HR-TEM) images of the NR junctions, detail of the chain in (f). g,h) The twinned *E-to-E* welding, and i,j) the perfect *E-to-E* welding. The white lines are guides for the eye to mark the orientation of the atomic planes. Scale bars: (a–f) 100 nm, (g–j) 5 nm.

process and the welding of already-assembled NRs take place simultaneously. Hence, the peak at 900 nm in the absorbance spectrum (Figure 1a) develops due to the contributions of the LPR of both: the trimers formed by not yet welded NRs and the new NRs of higher aspect ratio formed by the welding of a dimer.

As mentioned above, the key for the welding of chemically produced NPs is to obtain atomically clean surface by removing their capping molecules, here the CTAB bilayer.<sup>[7,9]</sup> The *E-to-E* NR welding indicates a preferential removal of the CTAB bilayer from the NR tips rather than from their sides. The geometrical

and crystallographic anisotropy of the AuNRs (Supporting Information), together with the preferential bounding of the CTAB on the NR sides<sup>[18]</sup> and the more fluxional and loosely packed structure of CTAB at the NR tips,<sup>[19]</sup> suggest the possibility of different surface chemistry taking place at the tips of the AuNRs as compared with their sides. The factors that could collaborate for the surface cleaning process are: i) the desorption of the outer layer of CTAB when the NRs are in a CTAB-free environment, ii) the penetration of water molecules at the interface between the gold surface and the head group of the cationic surfactant monolayers physisorbed on it,<sup>[20]</sup> and iii) the interaction between polymer and CTAB molecules, which could induce a progressive depletion of CTAB at the NR surface.<sup>[21,22]</sup>

It is well known that ionic surfactants can strongly interact with neutral polymers in solution,<sup>[20]</sup> and this interaction is accentuated when the polymer possesses some hydrophobic part on which the surfactant binds. More precisely, it has been shown that CTAB surfactants interact with both neutral polyethylene oxide (PEO) and polypropylene oxide (PPO) polymers.<sup>[22]</sup> On these basis, and noting the chemical structure of the polymers used containing certain number of PO groups, we have envisaged a similar strong interaction between CTAB and our copolymers. To prove the interaction between CTAB surfactant and poly(ethylene oxide-*st*-propylene oxide), measurements of conductimetry have been performed at room temperature by pouring drop by drop small amounts of a copolymer solution in a CTAB solution (Figure S2, Supporting Information). For both copolymers used in the present study, the critical aggregation concentration observed for CTAB/copolymer complex was smaller than the critical micellization concentration for CTAB alone. These results are in agreement with those observed for PEO and PPO polymers in interaction with CTAB surfactants.<sup>[22]</sup> Moreover, in an aqueous environment containing hydrophobic molecules, the

hydrophobic region of the CTAB bilayer has the ability to concentrate the hydrophobic molecules from solution.<sup>[23,24]</sup>

Fourier transform infrared spectroscopy (FTIR) (Figure S3a, Supporting Information) indicates the presence of polymer by the appearance of peaks in the region from 1050 to 1400  $\text{cm}^{-1}$ . In the surface-enhanced Raman scattering (SERS) spectrum of the NR solution after the addition of polymer (Figure S3b, Supporting Information), besides the vibrational signatures of CTAB, the presence of polymer on the NR surface is indicated by several bands between 800 and 1400  $\text{cm}^{-1}$  corresponding to the polymer spectrum.

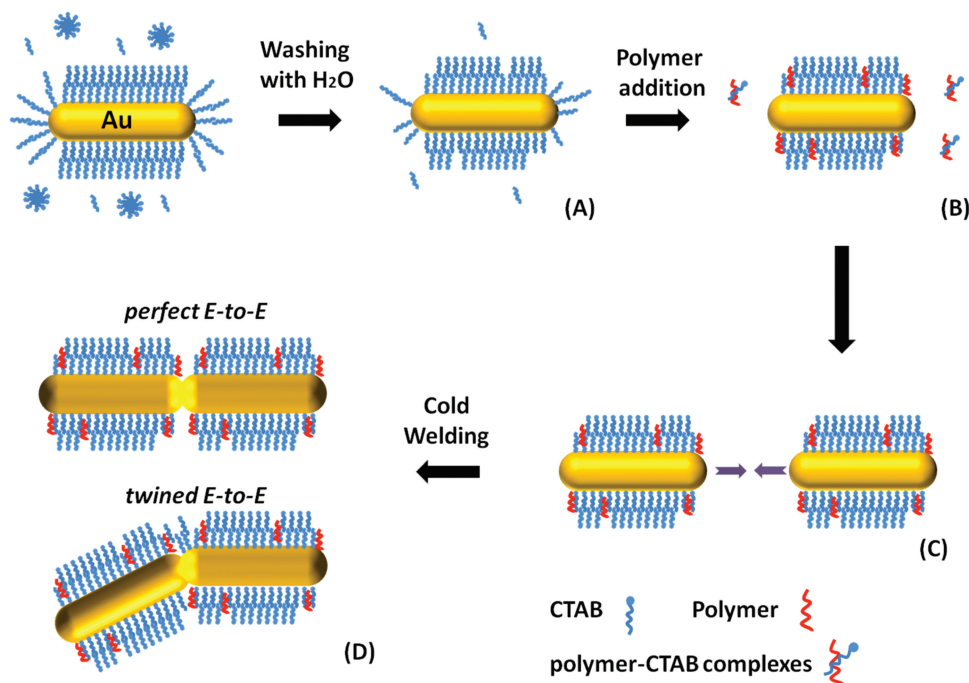


**Figure 3.** Scenario for the copolymer-induced cold welding of CTAB-capped AuNRs in water.

Taking in account, the results of HR-TEM, FTIR, SERS, the factors that could collaborate in the selective surface cleaning process, and the CTAB–polymer interaction, for the selective cold welding of colloidal NRs, we suggest the scenario shown in **Figure 3**. The initial process of NR washing reduces the total CTAB concentration (A). When the copolymer is introduced into the NR solution, it interacts with the free CTAB molecules in solution preventing their physisorption on the NR surface, extracts the weakly physisorbed CTAB from the NR tips and is integrated into the CTAB bilayer physisorbed on the NR sides (B). The interaction of the physisorbed CTAB with the polymer could be favored by the penetration of water molecules at the interface between the gold surface and the head group of the CTAB monolayers, weakening the strength of their physisorption on the NR<sup>[20]</sup> and hence favoring the cleaning of the NR surface. The NR tips lose at least partially their capping (C) and, when they come in proximity to other NRs, their welding takes place (D) by oriented attachment.<sup>[8]</sup>

The results of the start-stop-restart experiment (**Figure 4**) are in favor of the scenario suggested for surface cleaning due to the interplay between CTAB, water, and polymer. By adding CTAB, the consumption of isolated NRs is stopped (the absorbance at LPR remains constant, **Figure 4a**) as well as the production of chains (the absorbance at wavelengths longer than the LPR one remains constant, **Figure 4b**). This indicates an interruption of the assembling, due to the annihilation of the free copolymer action and the restoration of the colloidal stabilization by the excess of CTAB introduced in solution. It is noteworthy that the addition of CTAB does not lead to an increase in the number concentration of isolated NRs (**Figure 4a**), meaning that the already formed assemblies do not disassemble. After reducing the excess of CTAB by washing, the

assembling process restarts as soon as the polymer is introduced into the solution. This clearly indicates that the polymer-induced welding of AuNRs is based on its selective weakening of the NR capping.

The copolymer-induced NR welding is a cold welding since the experiments are performed in ambient conditions and no heating is involved. At the same time, this welding is different from the conventional cold welding since no mechanical force is applied for the NR surface cleaning of their capping molecules. It is remarkable, the fact that the *E-to-E* assembling leads mainly to the formation of chains, having interconnections of only two NRs, and not of three or more NRs at the same point. This can be explained by the predominant role of the dipolar forces in the assembling process. Liao et al.<sup>[8]</sup> have shown that the strong anisotropy of the potential energy distribution along an NP chain, when another NP is approaching it, favors the attachment of the new NP at the end of the chain and not at its middle.

In summary, we have shown that poly(EO-*st*-PO) copolymers can induce selective cold welding of CTAB-stabilized AuNRs in water, and we have suggested a scenario based on the NR surface cleaning. By monitoring the fast kinetics of UV–vis absorbance spectrum and performing electron microscopy, we have put in evidence the *E-to-E* assembling of AuNRs, which opens interesting outlooks for SERS and enhanced fluorescence applications.<sup>[6,25,26]</sup> For the first time, having as building blocks, CTAB-stabilized colloidal AuNRs, the formation of micrometer-length gold nanowires by nanoscale cold welding has been demonstrated. This is anticipated to be a possible future microfabrication technique with applications in the construction of interconnects for extremely dense logic circuits and flexible electronics,<sup>[27]</sup> as well as 3D scaffolds for tissue engineering.<sup>[28]</sup>

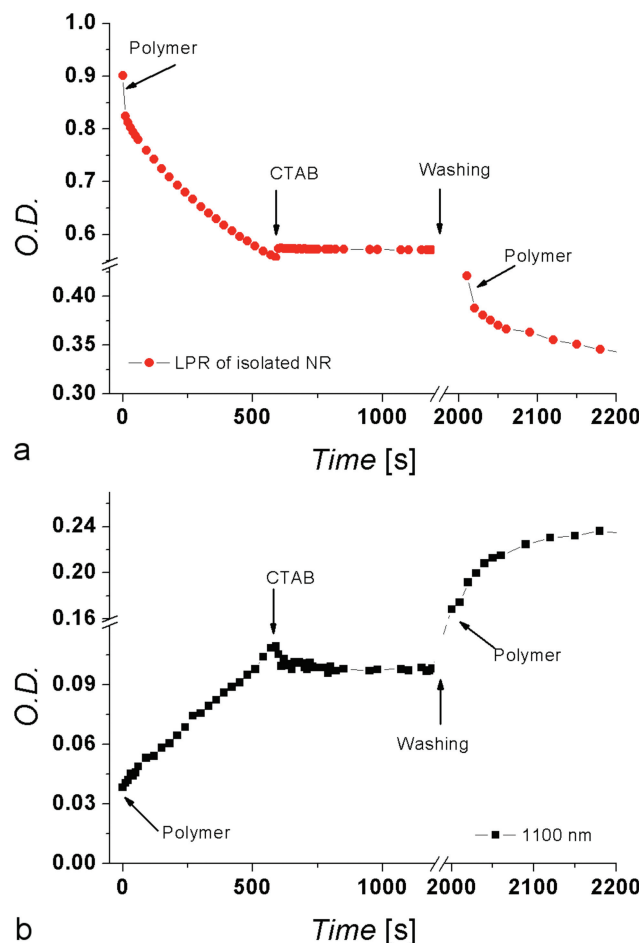


**Figure 4.** Evolution of the magnitude of a) the absorbance peak corresponding to the LPR of isolated NRs, b) the absorbance at 1100 nm, fingerprint of the formation of long chains, along the start-stop-restart test. The decrease (increase) of the absorbance corresponds to a decrease (increase) in the number concentration corresponding to the associated species (isolated NRs or chains).

## Experimental Section

**Materials:** Hydrogen tetrachloroaurate ( $\text{HAuCl}_4 \cdot 3\text{H}_2\text{O}$ ), sodium borohydride ( $\text{NaBH}_4$ ), ascorbic acid, CTAB, and silver nitrate ( $\text{AgNO}_3$ ) were used as purchased from Sigma-Aldrich. Poly(ethylene oxide-*st*-propylene oxide), poly( $\text{EO}_x$ -*st*- $\text{PO}_y$ ) copolymers, JEFFAMINE M600 and M1000, with designed molar masses of  $600 \text{ g mol}^{-1}$  and  $1000 \text{ g mol}^{-1}$  and ethylene oxide/propylene oxide ratios (EO/PO) of 1/9 and 19/3, respectively, were purchased from Huntsman Performance Products, USA. Ultrapure  $18 \text{ M}\Omega \text{ cm}$  water (MilliQ water; Millipore, France) was used for all solution preparations and experiments.

**NR Synthesis:** AuNRs ( $50 \text{ nm} \pm 5 \text{ nm}$  length and  $15 \text{ nm} \pm 3 \text{ nm}$  width) were synthesized by wet chemistry in water using a seed-mediated method in the presence of silver nitrate.<sup>[29,30]</sup>

**NR Washing:** Prior to use, the AuNR solution was submitted to three cycles of centrifugation and redispersion of the pellet in MilliQ water (Supporting Information).

**Optical Absorbance Kinetics:** Copolymer solution ( $200 \mu\text{L}$ ,  $0.1 \times 10^{-3} \text{ M}$ ), M600, or M1000, was added over purified AuNR solution ( $2 \text{ mL}$ ,  $0.7 \times 10^{-9} \text{ M}$ ) and the evolution of the optical absorbance spectra was monitored under continuous stirring (300 rpm, 8 mm length stirrer in a 1 cm cuvette) till the establishment of a “steady” spectrum. The optical absorbance measurements were carried out with a UV-vis

Hewlett-Packard 8453 spectrophotometer from 200 to 1100 nm. The experiments in which the addition of copolymer solution to the purified AuNR solution was performed without stirring lead to the same results: formation of micrometric length gold nanowires.

**Transmission Electron Microscopy:** Images of drop-casted NR solution on Formvar/carbon-coated copper grids (300/400 mesh), dried in air, were performed with a Philips CM120 electron microscope and HRTEM images were registered with a JEOL 2010 field electron gun microscope operating at an acceleration voltage of 200 kV.

**FTIR:** FTIR spectra were recorded at room temperature on a Bruker IFS 25.

**Fourier Transform Raman:** FT-Raman spectra were recorded at room temperature on an FT-Raman spectrometer Bruker IFS 66 interferometer coupled to a Bruker FRA 106 Raman module equipped with an Nd:YAG laser (1064 nm excitation).

**Start-Stop-Restart Experiment:** At a given time during the NR assembling, induced by the copolymer, CTAB solution ( $100 \mu\text{L}$ ,  $0.1 \text{ M}$ ) was added over the 2.2 mL NR solution with copolymer. After the establishment of the “steady” spectrum, the solution was washed (Supporting Information) and into the resulting “restart-solution” was added again copolymer solution ( $200 \mu\text{L}$ ,  $0.1 \times 10^{-3} \text{ M}$ ).

## Supporting Information

Supporting Information is available from the Wiley Online Library or from the author.

## Acknowledgements

This work was financially supported by Région Ile-de-France. The authors also thank S. Droniou for help with NR synthesis, L. Houel-Renault, D. Jaillard and X. Xu for assistance with TEM and HRTEM images, and H. Remita and N. Lequeux for fruitful discussions.

Received: January 22, 2013

Revised: March 13, 2013

- [1] K. Liu, N. Zhao, E. Kumacheva, *Chem. Soc. Rev.* **2011**, *40*, 656.
- [2] a) Z. Nie, A. Petukhova, E. Kumacheva, *Nat. Nanotechnol.* **2010**, *5*, 15; b) I. Mannelli, M. P. Marco, *Anal. Bioanal. Chem.* **2010**, *398*, 2451; c) C. De M. Donega, *Chem. Soc. Rev.* **2011**, *40*, 1512; d) J. Sharma, T. Imae, *J. Nanosci. Nanotechnol.* **2009**, *9*, 19.
- [3] a) K. Jain, S. Eustis, M. A. El-Sayed, *J. Phys. Chem. B* **2006**, *110*, 18243; b) K. M. Mayer, J. H. Hafner, *Chem. Rev.* **2011**, *111*, 3828.
- [4] A. Lukach, K. Liu, H. Therien-Aubin, E. Kumacheva, *J. Am. Chem. Soc.* **2012**, *134*, 18853.
- [5] a) X. Z. Nie, D. Fava, E. Kumacheva, S. Zou, G. C. Walker, M. Rubinstein, *Nat. Mater.* **2007**, *6*, 609; b) W. He, S. Hou, X. Mao, X. Wu, Y. Ji, J. Liu, X. Hu, K. Zhang, C. Wang, Y. Yang, Q. Wang, *Chem. Commun.* **2011**, 5482; c) S. Zhang, X. Kou, Z. Yang, Q. Shi, G. D. Stucky, L. Sun, J. Wang, C. Yan, *Chem. Commun.* **2007**, 1816; d) X. Hu, W. Cheng, T. Wang, E. Wang, S. Dong, *Nanotechnology* **2005**, *16*, 2164; e) T. Jain, R. Roodbeen, N. E. A. Reeler, T. Vosch, K. J. Jensen, T. Bjørnholm, K. Nørgaard, *J. Colloid Interface Sci.* **2012**, *376*, 83.
- [6] L. Zhong, X. Zhou, S. Bao, Y. Shi, Y. Wang, S. Hong, Y. Huang, X. Wang, Z. Xie, Q. Zhang, *J. Mater. Chem.* **2011**, *21*, 14448.
- [7] M. A. van Huis, L.T. Kunneman, K. Overgaag, Q. Xu, G. Pandraud, H. W. Zandbergen, D. Vanmaekelbergh, *Nano Lett.* **2008**, *8*, 3959.

- [8] a) H.-G. Liao, L. Cui, S. Whitelam, H. Zheng, *Science* **2012**, 336, 1011; b) D. Li, M. H. Nielsen, J. R. I. Lee, C. Frandsen, J. F. Banfield, J. J. De Yoreo, *Science* **2012**, 336, 1014.
- [9] Y. Lu, J. Y. Huang, C. Wang, S. Sun, J. Lou, *Nat. Nanotechnol.* **2010**, 5, 218.
- [10] E. C. Garnett, W. Cai, J. J. Cha, F. Mahmood, S. T. Connor, M. G. Christoforo, Y. Cui, M. D. McGehee, M. L. Brongersma, *Nat. Mater.* **2012**, 11, 241.
- [11] G. S. Ferguson, M. K. Chaudhury, G. B. Sigal, G. M. Whitesides, *Science* **1991**, 253, 776.
- [12] K.G. Thomas, S. Barazzouk, B. I. Ipe, S. T. S. Joseph, P. V. Kamat, *J. Phys. Chem. B* **2004**, 108, 13066.
- [13] A. M. Funston, C. Novo, T. J. Davis, P. Mulvaney, *Nano Lett.* **2009**, 9, 1651.
- [14] A. M. Funston, C. Novo, T. J. Davis, P. Mulvaney, *Phil. Trans. R. Soc. A* **2011**, 369, 3472.
- [15] Y. Wang, A. E. III DePrince, S. K. Gray, X.-M. Lin, M. Pelton, *J. Phys. Chem. Lett.* **2010**, 1, 2692.
- [16] Y. Min, M. Akbulut, K. Kristiansen, Y. Golan, J. Israelachvili, *Nat. Mater.* **2008**, 7, 527.
- [17] X. Huang, S. Neretina, M. A. El-Sayed, *Adv. Mater.* **2009**, 21, 4880.
- [18] N. R. Jana, L. Gearheart, S. O. Obare, C. J. Murphy, *Langmuir* **2002**, 18, 922.
- [19] C. J. Orendorff, T. M. Alam, D. Y. Sasaki, B. C. Bunker, J. A. Voigt, *ACS Nano* **2009**, 3, 971.
- [20] A. R. Godfrey Alig, M. Akbulut, Y. Golan, J. Israelachvili, *Adv. Funct. Mater.* **2006**, 16, 2127.
- [21] J. C. T. Kwak, in *Polymer-Surfactant Systems. Surfactant Sciences Series, Vol 77*, (Ed: J. C. T. Kwak), Marcel Dekker, New York **1998**.
- [22] a) F. M. Witte, J. B. F. N. Engberts, *J. Org. Chem.* **1987**, 52, 4767; b) M. L. Sierra, E. Rodenas, *J. Phys. Chem.* **1993**, 97, 12387; c) L. Meunier, K. Ballerat-Buserolles, G. Roux-Desgranges, A. H. Roux, *J. Thermal Anal.* **1998**, 54, 271; d) F. M. Witte, J. B. F. N. Engberts, *Colloids Surf.* **1989**, 36, 417.
- [23] C. J. Murphy, L. B. Thompson, A. M. Alkilany, P. N. Sisco, S. P. Boulos, S. T. Sivapalan, J. A. Yang, D. J. Chernak, J. Huang, *J. Phys. Chem. Lett.* **2010**, 1, 2867.
- [24] J. Y. Wu, J. H. Harwell, E. A. Orear, *Langmuir* **1987**, 3, 531.
- [25] G. Kawamura, Y. Yang, M. Nogami, *Appl. Phys. Lett.* **2007**, 90, 261908.
- [26] H. Feng, Y. Yang, Y. You, G. Li, J. Guo, T. Yu, Z. Shen, T. Wu, B. Xing, *Chem. Commun.* **2009**, 1984.
- [27] E. M. Freer, O. Grachev, X. Duan, S. Martin, D. P. Stumbo, *Nat. Nanotechnol.* **2010**, 5, 525.
- [28] a) T. Dvir, B. P. Timko, M. D. Brigham, S. R. Naik, S. S. Karajanagi, O. Levy, H. Jin, K. K. Parker, R. Langer, D. S. Kohane, *Nat. Nanotechnol.* **2011**, 6, 720; b) T. Dvir, B. P. Timko, D. S. Kohane, R. Langer, *Nat. Nanotechnol.* **2011**, 6, 13.
- [29] T. K. Sau, C. J. Murphy, *Langmuir* **2004**, 20, 6414.
- [30] a) E. Carbó-Argibay, B. Rodríguez-González, S. Gómez-Graña, A. Guerrero-Martínez, I. Pastoriza-Santos, J. Pérez-Juste, L.M. Liz-Marzán, *Angew. Chem. Int. Ed.* **2010**, 49, 9397; b) L. Vigderman, B. P. Khanal, E. R. Zubarev, *Adv. Mater.* **2012**, 24, 4811.